

Melt season duration on Canadian Arctic ice caps, 2000–2004

L. Wang,¹ M. J. Sharp,¹ B. Rivard,¹ S. Marshall,² and D. Burgess¹

Received 1 July 2005; revised 30 August 2005; accepted 2 September 2005; published 7 October 2005.

[1] The extent and duration of summer melt on ice caps in the Queen Elizabeth Islands (QEI), Nunavut, Canada, in 2000–2004 were mapped using enhanced resolution QuikSCAT (QSCAT) scatterometer images. The mean melt duration depends mainly on surface elevation and distance from Baffin Bay. Over most ice caps, inter-annual variations in melt duration and the variation in melt duration with elevation are closely related to variations in the July 500 hPa height over the QEI. Pressure-related variability in the vertical gradient of near-surface air temperature appears to be a major control on the inter-annual variations in average melt duration. **Citation:** Wang, L., M. J. Sharp, B. Rivard, S. Marshall, and D. Burgess (2005), Melt season duration on Canadian Arctic ice caps, 2000–2004, *Geophys. Res. Lett.*, 32, L19502, doi:10.1029/2005GL023962.

1. Introduction

[2] Melting of all glaciers and ice caps (excluding the Antarctic and Greenland ice sheets) would raise sea level by ~0.5 m [Church *et al.*, 2001]. 46% of the area of these glaciers and ice caps is in the Arctic [Dyurgerov, 2002], where there was strong warming in the 20th century [Johannessen *et al.*, 2004]. General Circulation Model simulations predict that this trend will continue and likely increase in the 21st century due to anthropogenic forcing [Houghton *et al.*, 2001]. It is therefore important to understand how and why the extent and volume of glacier ice in the Arctic have changed in the recent past.

[3] There is over 110,000 km² of glacier ice in Canada's Queen Elizabeth Islands (QEI) [Koerner, 2002]. Variations in summer melt drive the inter-annual variability in glacier mass balance in the QEI [Koerner, 2002], so there is a strong interest in monitoring summer melt across the region. Satellite-borne Ku- and C-band radar scatterometers have been used to detect melt on the Greenland Ice Sheet [Wismann, 2000; Nghiem *et al.*, 2001; Steffen *et al.*, 2004]. Smith *et al.* [2003] used this method to detect melt within single pixels on several small Arctic ice caps, but could not undertake synoptic melt mapping because of the coarse resolution of the sensors (~25 km). In this study, enhanced resolution data from QSCAT [Long and Hicks, 2005] were used to detect the dates of melt onset and freeze-up, and determine annual melt extent and duration across all major ice caps in the QEI for the period 2000–2004. The results provide a measure of variability in summer climate over ice-covered areas remote from long-term weather

stations and may prove useful in the development of methodologies for up-scaling site-specific measurements of glacier mass balance [Koerner, 2002] to the regional ice cover.

2. Methods

2.1. Data

[4] The SeaWinds scatterometer on QSCAT makes measurements at Ku-band frequency with two constant incidence angles: 46° at H-pol over a 1400 km swath, and 54° at V-pol over an 1800 km swath. The resolution of the original data is low. Due to its wide swath and orbit geometry, however, QSCAT observes the Polar Regions multiple times each day, allowing reconstruction of surface backscatter at finer spatial resolution using the Scatterometer Image Reconstruction (SIR) algorithm [Long and Hicks, 2005]. Ascending and descending pass images produced with this algorithm are available daily for the Arctic since July 1999. These images have a nominal pixel spacing of 2.225 km and an estimated effective resolution of 5 km [Long and Hicks, 2005]. Due to ascending-to-descending swath overlap and day boundary effects in the Polar Regions, there is large temporal variability in the measurements used to construct each (ascending/descending) image [Hicks and Long, 2005]. The majority of effective measurement times (local) over the QEI are 10 pm for descending pass images, and 2 am for ascending pass images. Since ice caps are more likely to be melting at 10 pm, descending pass images (H-pol) were used to detect melt in this study.

[5] 1:250,000 NTDB (National Topographic Data Base) shapefiles of permanent ice were used to extract ice pixels from the QSCAT data. These shapefiles are based on aerial photographs taken in 1959/1960, and many glaciers and ice caps have changed significantly since then. The ice mask thus includes many mixed pixels along the ice margins and in areas surrounding nunataks. Landsat7 ETM+ (30 m) or MODIS (250 m) images from 1999 to 2002 were used to identify these mixed pixels and remove them from the ice mask.

[6] To validate the use of QSCAT images for detecting surface melt, 25 air temperature loggers (either Onset HOBO H8-PRO loggers or Veriteq SP2000 temperature-relative humidity loggers with an accuracy of ±0.25°C) were deployed at elevations from 130–2010 m on the Prince of Wales (POW) Icefield, Ellesmere Island, from 2001–2003. Sensors were installed in Onset radiation shields (without ventilation) and recorded near-surface (1–1.5 m) air temperatures at 30-minute intervals (S. J. Marshall *et al.*, Surface temperature lapse rate variability on the Prince of Wales Icefield, Ellesmere Island, Canada: Implications for regional-scale downscaling of temperature, submitted to *International Journal of Climatology*, 2005, hereinafter referred to as Marshall *et al.*, submitted manuscript, 2005).

¹Earth and Atmospheric Sciences, University of Alberta, Edmonton, Alberta, Canada.

²Department of Geography, University of Calgary, Calgary, Alberta, Canada.

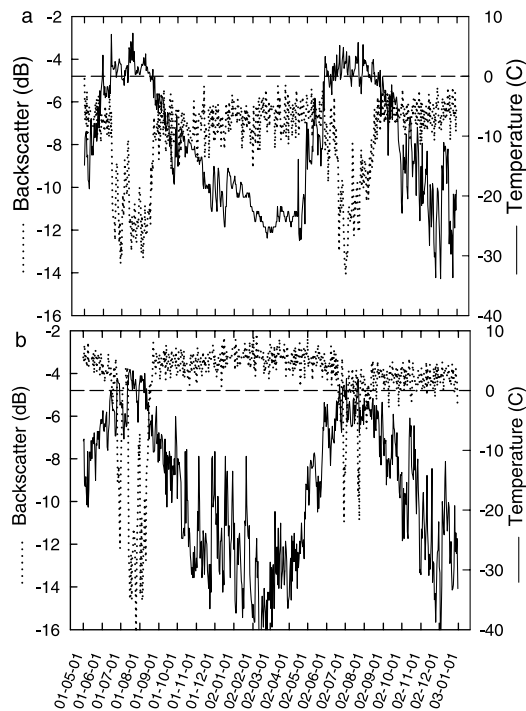


Figure 1. Time series of QSCAT σ^0 and surface air temperature during 2001–2002 for 2 locations on POW Icefield, (a) 78.68°N, 74.96°W, 400 m a.s.l., (b) 78.61°N, 78.63°W, 1300 m a.s.l.

2.2. Melt Threshold and Melt Detection

[7] The basis for melt mapping is the reduction in Ku-band radar backscatter (σ^0) that occurs during the melt season. Liquid water in snow dramatically increases microwave absorption and masks out subsurface scattering, resulting in decreased σ^0 at the onset of snowmelt [Ulaby *et al.*, 1981]. Transient increases in σ^0 occur during subsequent periods of refreezing, but σ^0 falls again if snowmelt resumes. At low elevations, the snow pack may be removed completely in summer, exposing glacier ice. Backscatter may then increase over time due to the relative roughness of the ice surface, but detailed comparisons of σ^0 and air temperature records from POW indicate that these increases are significantly less than those associated with refreezing.

[8] During winter (December to February), mean σ^0 values (W_{mn}) increase with elevation, while the standard deviations (W_{sd}) decrease (auxiliary Figure A1¹). Since dry snow is almost transparent at Ku-band frequency [Ulaby *et al.*, 1981], this is mainly due to elevation dependent differences in the physical properties (grain size, surface roughness, density, ice layers) of near surface snow and firn at the end of the previous summer. Nevertheless, this result implies that the magnitude of σ^0 that indicates melting during the following summer will vary with W_{mn} and W_{sd} . Two dynamic thresholds were therefore used to detect melt in each pixel:

$$M_1 = W_{mn} - a(W_{sd})^{-b} \quad (1)$$

$$M_2 = cM_1 \quad (2)$$

Here a , b , and c are user defined constants. Using trial and error and the air temperature records, optimal values for a , b , and c were identified as: $a = c = 1.3$, $b = -1.1$. For each pixel, all periods when either (A) σ^0 remained below M_1 for 3 or more consecutive days, or (B) σ^0 dropped below M_2 for 1 day, were categorized as melt days. Step (A) eliminates possible “false starts” in melt onset; and step (B) makes it possible to capture short periods of melt at high elevations on the ice caps. The first melt day and last melt day plus one were used as melt onset and freeze-up dates respectively. The number of melt days in each pixel was determined as the time period between melt onset and freeze-up minus the duration of any periods without melt within the melt season.

[9] At all elevations on POW, there is a close correspondence between the periods of decreased σ^0 (MD_{QS}) and positive air temperatures (MD_T) in the 20:00–23:00 time window (Figure 1). Linear regression gives $MD_{QS} = 0.9 MD_T + 9$ days ($r^2 = 0.78$, $P < 0.001$, standard error of the estimate = 10.1 days). There is also a good relationship between MD_{QS} and the annual positive degree-day total ($\Sigma PDD = 0.11 + 0.6036 MD_{QS} + 0.01430 MD_{QS}^2$, $r^2 = 0.74$, $p < 0.001$, standard error of the estimate = 20 PDD).

3. Results and Discussion

3.1. Melt Climatology

[10] Average melt onset dates range from late May to mid-July (Figure 2a), and freeze-up dates range from mid-July to early September (Figure 2b). Melt duration ranges from 1 day or less at high elevations to 100 days at low elevations in areas facing Baffin Bay in the southeast QEI (Figure 2c). For the whole QEI, the average is 37.7 days (standard deviation (s.d.) = 4.9 days, Table 1). Ice cap margins facing either Baffin Bay to the southeast or the Arctic Ocean to the northwest have significantly longer melt seasons than margins facing the interior of the QEI. Areas with longer melt seasons tend to have both earlier melt onset and later freeze-up dates.

[11] The spatial pattern of melt duration can be well explained in terms of surface elevation and distance from Baffin Bay (measured relative to 74.010°N, 75.042°W) – a

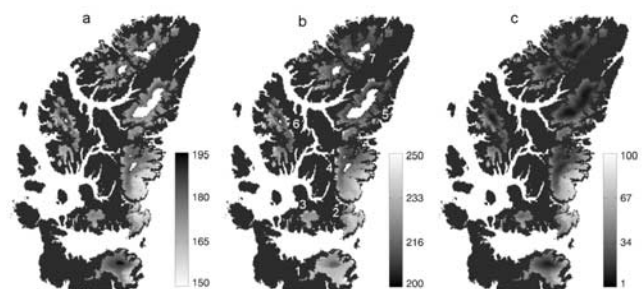


Figure 2. Melt climatology for the QEI for the period 2000–2004, (a) melt onset dates; (b) freeze-up dates; (c) the number of melt days. Anomalies in onset and freeze-up dates cannot be calculated for areas shown in white, as melt was not detected in these areas in all years. Numbers in (b) indicate major ice caps: 1~Devon; 2~Manson; 3~Sydkap; 4~POW; 5~Agassiz; 6~Axel Heiberg Island; 7~Northern Ellesmere Island. See color version of this figure in the HTML.

¹Auxiliary material is available at <ftp://ftp.agu.org/apend/gl/2005GL023962>.

Table 1. Average Melt Duration Over the Whole QEI and Each Major Ice Cap, for the Summers of 2000–2004^a

Ice Cap	Melt Duration, days							Mean Elevation, m	Area Above 1000 m, %	Correlation With 500 hPa
	2000	2001	2002	2003	2004	Mean	S.D.			
QEI	39.1	42.6	30.9	41.4	34.7	37.7	4.9	998	58	0.96
Devon	40.8	50.9	37.5	45.7	35.4	42.1	6.3	1080	56	0.93
Manson	61.6	63.4	62.4	57.6	63.4	61.7	2.4	585	4	-0.2
Sydkap	49.0	49.2	32.7	44.1	45.1	44.0	6.7	827	23	0.77
POW	47.6	53.9	40.1	51.0	44.7	47.4	5.4	967	49	0.95
Agassiz	29.8	32.6	16.2	29.8	22.9	26.3	6.7	1286	77	0.92
Axel Heiberg	40.4	39.0	31.8	40.4	36.0	37.5	3.7	1073	57	0.93
N. Ellesmere	31.4	32.7	23.9	37.1	26.6	30.3	5.2	1171	68	0.97

^aThe mean elevation and the percentage of area above 1000 m for each ice cap, and the correlation between melt duration and July 500 hPa height are also shown.

source of warm maritime air masses. Multiple regression gives: $MD_{QS} = 87.98 - 0.0346h - 0.0461x$ ($r^2 = 0.69$, $p < 0.001$), where h is surface elevation (m) and x is distance from Baffin Bay (m). The correlation with distance from Baffin Bay alone is -0.44 , while that with elevation is -0.80 , so surface elevation is the main influence on melt duration in the QEI. MD_{QS} ranges from 26.3 days (s.d. = 6.7 days) on the Agassiz Ice Cap to 61.7 days (s.d. = 2.4) on the Manson Icefield (Table 1). This is consistent with the mean elevations of the ice caps: 1286 m for Agassiz and 585 m for Manson.

3.2. Melt Anomalies

[12] For the whole QEI, the longest melt season was 2001 (42.6 days) and the shortest 2002 (30.9 days) (Table 1). The pattern for individual ice caps was similar (Table 1), although 2003 was the longest melt season on the Northern Ellesmere and Axel Heiberg Island ice caps, and the shortest season on the Manson Icefield. 2004 was the shortest melt season on the Devon Ice Cap. In relatively cool years, like 2002 and 2004, no melt was detected in some high elevation areas of Ellesmere Island and Axel Heiberg Island (Figure 2).

[13] In the southeast QEI, the melt duration anomalies in 2001 and 2002 were of opposite sign at high and low elevations (Figure 3, auxiliary Figure A2). At low elevations, the anomalies were extremely negative in 2001 and extremely positive in 2002 (i.e. the low elevation anomalies were of opposite sign to the anomalies for the ice caps as a whole). On POW, the decrease in melt duration with increasing elevation was almost linear in 2001 (Figure 4). In 2002 the melt duration decreased abruptly between 700 m

(68 days) and 1100 m (29 days), resulting in a much steeper average rate of decrease of melt duration with increasing elevation. Consistent with this, lapse rates in daily mean surface air temperature in June–August were $-3.7^\circ\text{C km}^{-1}$ in 2001 and $-5.1^\circ\text{C km}^{-1}$ in 2002 (Marshall et al., submitted manuscript, 2005). In 2001, the melt duration at elevations below 700 m was less than in the generally shorter melt season of 2002. This suggests that in some years, like 2002, the temperature regimes of the high and low elevation regions of the Icefield are partially decoupled, while in other years, like 2001, they are more closely related. The correlation coefficient between the June–August daily mean air temperatures at stations at 130 m and 1300 m was 0.74 in 2001, but only 0.56 in 2002.

[14] Alt [1987] found that high melt years on QEI ice caps were associated with the intrusion of a ridge into the QEI at all levels in the troposphere, while low melt years were associated with the maintenance of a deep cold trough across Ellesmere Island and down Baffin Bay, which resulted in northwest flow off the Polar Ocean. In addition, on POW, less negative vertical gradients in daily mean surface air temperature (2001) are associated with high pressure and anticyclonic flow, while more negative gradients (2002) are associated with low pressure and generally cyclonic flow (Marshall et al., submitted manuscript, 2005). It was thus hypothesized that melt season duration would vary systematically with geopotential height over the QEI. Indeed, the correlation between the mean melt season duration over the QEI and the mean July 500 hPa height over the region $74\text{--}83^\circ\text{N}$, $70\text{--}92^\circ\text{W}$ (as derived from the NCEP-CDAS Reanalysis [Kalnay et al., 1996]) was $+0.96$ (Table 1). Similar relationships were found for all the

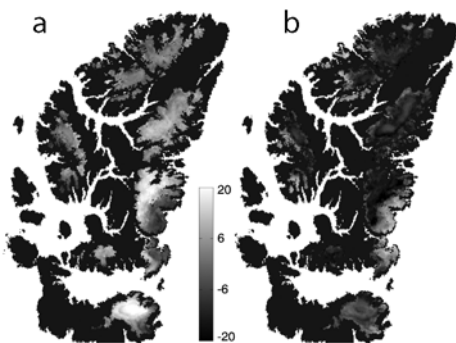


Figure 3. Anomalies in melt duration over QEI relative to the 2000–2004 climatology for the summers of (a) 2001 and (b) 2002. See color version of this figure in the HTML.

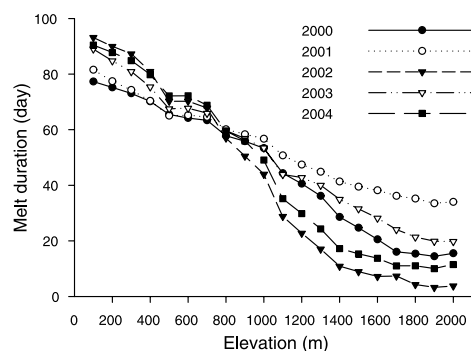


Figure 4. Average melt duration in each 100 m elevation band on POW Icefield in the summers of 2000–2004.

individual ice caps except the Manson Icefield and, possibly, Sydkap, which have low mean surface elevations and relatively small areas above 1000 m (Table 1). Although these results are based on only 5 years of data, they suggest that the less negative surface air temperature gradients associated with high mean geopotential heights result in longer than average melt seasons at higher elevations on the QEI ice caps, and in longer melt seasons overall. In contrast, lower mean geopotential heights are associated with more negative surface air temperature gradients, shorter melt seasons at high elevations, and shorter melt seasons overall.

[15] In the QEI, 2002 was the shortest melt season in the period 2000–2004. On the Greenland Ice Sheet, however, unusually extensive melt in northeast Greenland made 2002 the year with the most extensive melt in the period 1979–2003 [Steffen *et al.*, 2004]. NCEP-CDAS Reanalysis data reveal a positive 500 hPa geopotential height anomaly over northeast Greenland in June and July 2002, while the anomaly was negative over the QEI. This suggests that changes in melt extent and duration in the QEI and northern Greenland may have a common relationship to changes in the distribution of atmospheric mass.

4. Summary and Conclusions

[16] The extent and duration of summer melt on the QEI ice caps from 2000–2004 were mapped using enhanced resolution QSCAT backscatter time-series. The 5-year mean melt duration pattern was largely a function of surface elevation, with shorter melt seasons at higher elevations. No melt was detected over some high-elevation regions in 2002 and 2004. For monitoring sites on the POW Icefield, QSCAT derived melt durations correspond well with those derived from air temperature measurements, and are well correlated with the annual positive degree-day total. This suggests that it may be possible to use maps of melt duration to derive positive degree-day fields that could be used to compute summer melt volume using temperature index melt models.

[17] The annual mean melt duration over the larger ice caps is positively correlated with the local 500 hPa height. In a given year, however, the sign of melt duration anomalies may be opposite at high and low elevations on an ice cap. This phenomenon appears to be linked to pressure-related variations in the vertical gradient of surface air temperature over the ice caps, which is more negative in years with relatively low pressure. Thus, in high-pressure years, ice caps with relatively large areas at high elevations experience

longer than average melt seasons, which increases the mean melt duration over the whole ice cap. The mean melt duration over these ice caps can therefore be inversely correlated to the duration at elevations near sea level.

[18] **Acknowledgments.** This research was supported financially by the Meteorological Service of Canada's CRYSYS program, and logistically by the Polar Continental Shelf Project, Natural Resources Canada. The Microwave Earth Remote Sensing Laboratory, Brigham Young University provided the QSCAT data. We thank D.G. Long for his help with reading the QSCAT data and for discussions. The Nunavut Research Institute and the peoples of Grise Fjord and Resolute Bay gave permission to conduct the field component of this research.

References

- Alt, B. T. (1987), Developing synoptic analogues for extreme mass balance conditions on Queen Elizabeth Island ice caps, *J. Clim. Appl. Meteorol.*, *26*, 1605–1623.
- Church, J., et al. (2001), Changes in sea level, in *Climate Change 2001: The Scientific Basis*, edited by J. T. Houghton et al., pp. 639–693, Cambridge Univ. Press, New York.
- Dyrugerov, M. (2002), Glacier mass balance and regime: Data of measurements and analysis, *Occas. Pap.* *55*, Univ. of Colo., Boulder.
- Hicks, B. R., and D. G. Long (2005), Improving temporal resolution of SIR images for QuikSCAT in the polar regions, report, Brigham Young Univ., Provo, Utah.
- Houghton, J. T., et al. (Eds.) (2001), *Climate Change 2001: The Scientific Basis*, Cambridge Univ. Press, New York.
- Johannessen, O. M., et al. (2004), Arctic climate change: Observed and modelled temperature and sea-ice variability, *Tellus, Ser. A*, *56*, 328–341.
- Kalnay, E., et al. (1996), The NCEP/NCAR 40-year reanalysis project, *Bull. Am. Meteorol. Soc.*, *77*, 437–471.
- Koerner, R. M. (2002), Glaciers of the High Arctic Islands, in *Satellite Image Atlas of Glaciers of the World: Glaciers of North America—Glaciers of Canada*, edited by R. S. Williams Jr. and J. G. Ferrigno, *U.S. Geol. Surv. Prof. Pap.* *1386-J*, j111–j146.
- Long, D. G., and B. R. Hicks (2005), Standard BYU QuikSCAT/SeaWinds land/ice image products, report, Brigham Young Univ., Provo, Utah.
- Nghiem, S. V., K. Steffen, R. Kwok, and W. Y. Tsai (2001), Detection of snowmelt regions on the Greenland ice sheet using diurnal backscatter change, *J. Glaciol.*, *47*, 539–547.
- Smith, L. C., Y. Sheng, R. R. Forster, K. Steffen, K. E. Frey, and D. E. Alsdorf (2003), Melting of small Arctic ice caps observed from ERS scatterometer time series, *Geophys. Res. Lett.*, *30*(20), 2034, doi:10.1029/2003GL017641.
- Steffen, K., S. V. Nghiem, R. Huff, and G. Neumann (2004), The melt anomaly of 2002 on the Greenland Ice Sheet from active and passive microwave satellite observations, *Geophys. Res. Lett.*, *31*, L20402, doi:10.1029/2004GL020444.
- Ulaby, F. T., R. K. Moore, and A. K. Fung (1981), *Microwave Remote Sensing: Fundamentals and Radiometry*, Addison-Wesley, Boston, Mass.
- Wismann, V. (2000), Monitoring of seasonal snowmelt in Greenland with ERS scatterometer data, *IEEE Trans. Geosci. Remote Sens.*, *38*, 1821–1826.

D. Burgess, B. Rivard, M. J. Sharp, and L. Wang, Earth and Atmospheric Sciences, University of Alberta, Edmonton, AB, Canada T6G 2E3. (libo@ualberta.ca)

S. Marshall, Department of Geography, University of Calgary, Calgary, AB, Canada T2N 1N4.